Development of REBCO Thin Films Using MOCVD on Non-Standard Buffers and Substrates

Manoj Thevalappilly Paulose, Jithin Sai Sandra, Md Abu Sayeed, and Venkat Selvamanickam, *Fellow, IEEE*

***Abstract*—Rare Earth Barium Copper Oxide (REBCO) superconducting thin films on dielectric substrates are being developed for microwave and radio frequency applications such as transmission lines for quantum computing. Our group previously demonstrated the growth of REBCO thin films on short, flexible, yttria-stabilized-zirconia (YSZ) substrates. In this study, we report high-quality REBCO films on 12-cm-long flexible YSZ substrates. We planarized the surface of 40-μm-thick flexible YSZ substrate by vertical dip coating in n-propanol solution to achieve average surface roughness R_a <1 nm over 12 cm. We deposited a biaxially-textured magnesium oxide (MgO) template on a yttria seed layer using Ion Beam Assisted Deposition (IBAD) on flexible YSZ. Then, we deposited a 120-nm-thick MgO layer and a 120-nm-thick $LaMnO_3$ (LMO) cap layer. The out-of-plane and in-plane texture values of the LMO films were 3.9° and 6.9° respectively. REBCO films of a thickness of 350 nm were grown on these 12-cm-long flexible YSZ substrates by metal organic chemical vapor deposition (MOCVD) and a critical current density (J_c) of 1.06 MA/cm^2 was achieved at 77 K, 0 T. We are also developing an electrically conductive buffer architecture for defect-tolerant REBCO tapes, to shunt current from the REBCO film to substrate. This buffer architecture is based on conductive titanium nitride buffer on Hastelloy C276 substrate, with an oxide cap layer deposited by magnetron sputtering. REBCO films, about 350 nm thick, have been grown by MOCVD on this buffer architecture with a J_c greater than 1 MA/cm^2 at 77 K, self-field. Texture, microstructure, composition and critical current density of REBCO tapes on electrically conductive buffers will be presented.**

***Index Terms*—Conductive buffer, dielectric substrate, flexible electronics, MOCVD, rare earth barium copper oxide (REBCO), RF application, quantum computing.**

Received 25 September 2024; revised 18 November 2024 and 26 November 2024; accepted 2 December 2024. Date of publication 23 December 2024; date of current version 3 January 2025. The work of author Venkat Selvamanickam was supported by AMPeers. This work was supported in part by U.S. Naval Sea Systems Command Small Business Technology Transfer award under Grant N68335-23-C-0228 through AMPeers LLC and in part by the Office of Naval Research award under Grant N00014-21-1-2429 *(Manoj Thevalappilly Paulose and Jithin Sai Sandra contributed equally to this work.) (Corresponding author: Manoj Thevalappilly Paulose.)*

Manoj Thevalappilly Paulose, Md Abu Sayeed, and Venkat Selvamanickam are with the Mechanical Engineering Department, University of Houston, Houston, TX 77204 USA, also with the Advanced Manufacturing Institute, University of Houston, Houston, TX 77023 USA, and also with the Texas Center for Superconductivity, University of Houston, Houston, TX 77204 USA (e-mail: manojtpoulose@gmail.com; sayeedrasel29@gmail.com; selva@uh.edu).

Jithin Sai Sandra is with AMPeers LLC, Houston, TX 77059 USA (e-mail: jithinsaisandra@gmail.com).

Color versions of one or more figures in this article are available at https://doi.org/10.1109/TASC.2024.3513942.

Digital Object Identifier 10.1109/TASC.2024.3513942

I. Introduction

REBCO (Rare Earth Barium Copper Oxide) coated conductors are very promising superconductors, because of their high critical temperature and irreversibility field. These superconductors can function well in magnetic fields over a wide temperature range (4.2 K to 77 K) [1]. REBCO superconductors are suitable for a variety of applications, such as power transmission cables [2], high-energy particle accelerators [3], radio frequency (RF) devices [4], motors [5], fusion energy systems [3], [6], generators [5], and superconducting magnetic energy storage devices [7]. REBCO coated conductors have been primarily developed on flexible metallic substrates, such as Ni-W [8] and Hastelloy [9].

The surface resistance (R_s) of REBCO is more than ten times lower than that of copper at 77 K and 10 GHz [1]. This reduced surface resistance is advantageous for various RF components, such as resonators [10], microstrip lines [11], microwave circuits [12], band-pass filters [13], radiation detectors [14], and superconducting quantum interference devices (SQUIDs) [15]. Surface resistance is more important in RF applications because RF currents are confined to a thin surface layer due to the skin effect, making surface properties critical for minimizing energy losses. Despite these benefits, REBCO coated conductors on flexible metallic substrates face significant challenges in RF applications due to substantial microwave losses caused by the metallic substrates. These losses, particularly pronounced in the megahertz (MHz) frequency range, result from alternating current (AC) losses induced by eddy currents in the metal [16]. Various research efforts have explored replacing metallic substrates with dielectric materials to reduce microwave losses. Single-crystal dielectric substrates, such as sapphire, and lanthanum aluminate ($LaAlO_3$) have primarily used for microwave applications but are not suitable for long, flexible transmission lines [16]. Recently, Obradors et al. demonstrated that Chemical Solution Deposition (CSD)-grown YBCO films with thicknesses up to 400 nm and critical current density (J_c) values of approximately 1.9 MA/cm^2 at 77 K can be achieved on $Ce_{1-x}Zr_xO_2$(CZO)/yttrium-stabilized zirconia/r-cut barely polished sapphire (BPS) substrates, offering a cost-effective option for superconducting fault current limiter (SFCL) devices [17]. Flexible polycrystalline yttria-stabilized-zirconia (YSZ) is an excellent non-metallic substrate for REBCO growth. Its low thermal conductivity, low dielectric constant, and strong chemical compatibility, along with its capability to endure temperatures up to 1200 °C, make YSZ a superior choice [18]. Previously, our

group demonstrated growth of REBCO superconducting film on YSZ dielectric substrate of 1 cm length using advanced metal–organic chemical vapor deposition (A-MOCVD) [19]. Later, we successfully extended REBCO thin films to 5-cm-long dielectric YSZ substrates using a conventional MOCVD tool [20]. These films exhibit a surface resistance of approximately 0.1 mΩ/square at 25 K and 9.4 GHz, with a high critical current density exceeding 1 MA/cm^2; [20].

In electric power and high magnetic field applications, uncontrolled quench is a problem due to localized heating at defects in long tapes [21]. Superconducting coils typically include insulated tape turns, which makes it difficult for heat to dissipate from the defective locations, which can cause a thermal runaway and a damage to the devices. Incorporating an electrically conductive buffer stack can help establish a reliable electrical contact between the thick metal substrate and overlaying high-temperature superconducting layer, improving stability during transient events [22]. By providing a lower resistive path during around defects, an electrically conductive buffer stack can improve both the reliability of superconducting tapes. Titanium Nitride (TiN) is a promising material as electrically-conductive buffer layer for REBCO films, offering a strong biaxial-texture, barrier to metal diffusion, and a thermal expansion coefficient compatible with REBCO [23]. However, TiN is highly susceptible to oxidation under the high deposition temperatures and oxidative conditions typical in MOCVD processes. An alternate electrically-conducting buffer layer that can resist oxidation in MOCVD conditions is needed for high-performance REBCO tapes.

This reports on the optimization of the growth of REBCO (RE: yttrium and gadolinium) superconductor films on long flexible YSZ substrates and on conductive buffer layers on metallic substrates. We report high-quality REBCO films grown on 12-cm-long flexible YSZ substrates and the development of REBCO film over conductive buffer architecture using titanium nitride on Hastelloy C276 metallic substrate.

II. Experimental Methods

A. Development of Buffer Layer

Commercially available flexible YSZ sheets (acquired from OASIS MATERIALS), measuring 18 cm × 6 cm with a thickness of 40 μm, were sliced into 1-cm-wide samples using laser slitting and used as substrates. These YSZ samples can be bent to a radius of 3-4 cm, demonstrating excellent substrate flexibility. These substrates were preprocessed using a Solution Deposition Process (SDP) in n-butanol-based solution reported previously.[18], [19]. We employed a dip-coating technique to planarize long-length samples. By optimizing the process, a smooth, glass-like surface was achieved after applying eight layers of dip coating.

The planarized YSZ samples were pre-etched with Ar+ ions to improve surface finish, followed by ion beam sputtering to grow an 8-nm-thick amorphous yttrium oxide (Y_2O_3) seed layer at ambient conditions. A biaxially-textured IBAD MgO layer (10 nm thick) was deposited using simultaneous sputter and assist ion sources, with real-time monitoring via Reflection High Energy Electron Diffraction (RHEED). Subsequently, a homoepitaxial magnesium oxide (MgO) layer and an $LaMnO_3$ (LMO) cap layer were deposited using reactive sputtering at 900 °C, as reported in previous work [19], [20].

An electrically-conductive buffer layer stack, consisting of niobium-doped strontium titanate ($SrTiO_3$) and aluminum-substituted titanium nitride (Ti_3AlN), was developed on standard Hastelloy C276 substrate using an RF magnetron sputtering system. The $SrTiO_3$ cap layer was sputter deposited onto the underlying Ti_3AlN layer, which exhibited an electrical resistivity of 43 μΩ cm at room temperature. The Ti_3AlN layer was deposited on an IBAD MgO template that includes yttrium oxide (Y_2O_3) and aluminum oxide (Al_2O_3) layers on electropolished Hastelloy C276. This textured buffer architecture provides a robust foundation for the subsequent growth of REBCO films. The detailed process for these buffer layers has been described elsewhere in this volume [24].

B. REBCO Growth

A custom-built reel-to-reel MOCVD equipment was used for growing REBCO films [20]. A solution of MOCVD precursors is injected into an evaporator. The precursor vapors are then transported to the reaction chamber by nitrogen carrier gas. A showerhead assembly is used to deliver precursor vapors and oxygen over the buffered substrate that is heated by conduction heating over a susceptor. After REBCO deposition, the samples are oxygenated at 500 °C for two hours. In addition to the flexible dielectric substrate, metallic substrate with electrically conductive buffer layers was used for the growth of REBCO [24].

C. Characterization

Crystallographic texture was examined using a 2D-X-ray Diffraction (XRD) (Bruker D8 GADDS) tool operating at 50 kV, 1000 mA, while in-situ texture monitoring during the IBAD process was done with RHEED. Atomic Force Microscopy (AFM) was used to determine the average surface roughness (R_a) of the planarized YSZ samples. Cross-sectional analysis was conducted using FEI 235 Focused Ion Beam (FIB), and surface morphology of the REBCO film was investigated with Scanning Electron Microscopy (SEM) (Axia ChemiSEM). Superconducting performance was assessed using Scanning Hall Probe Microscopy (SHPM) at 77 K, and the transport critical current (I_c) of REBCO tapes was measured using the four-probe method with a voltage criterion of 1 μV/cm. DC current was provided by a Lambda GEN-5000W power supply.

III. Results and Discussion

A. Growth of REBCO on Flexible YSZ Dielectric Substrate

Pre-processing bare YSZ substrates is crucial for high-quality buffer layers. While commercial YSZ has a surface roughness of 13-14 nm, an optimal roughness of around 1 nm is required for effective oxide buffer and REBCO film growth. [25]. After planarizing the YSZ substrates, we achieved a glass-like surface with an average roughness (R_a) below 2 nm, making them suitable for high-quality buffer and REBCO film growth. AFM

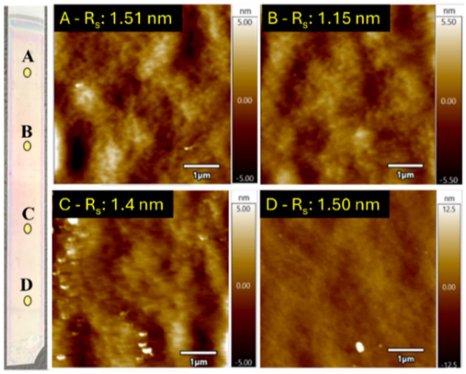

Fig. 1. (Left) Photograph of flexible YSZ sample with four marked locations selected for AFM analysis after planarization. (Right) AFM images corresponding to the four marked locations on the left image after eight layers of vertical dip coating planarization.

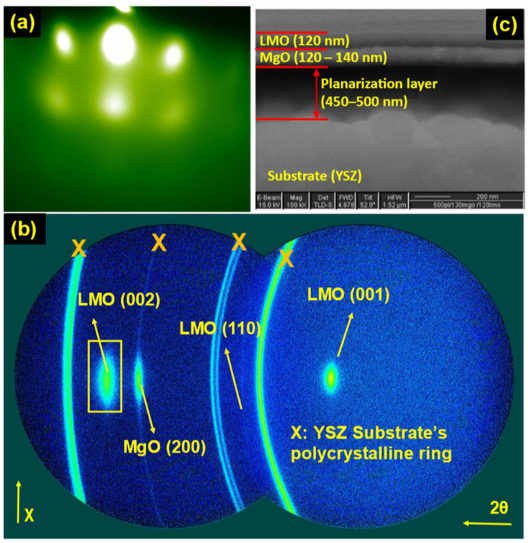

Fig. 2. (a) RHEED pattern of IBAD MgO (200) film during deposition on flexible YSZ, (b) 2D-XRD scan of buffer layer on flexible YSZ. (c) SEM cross-section of the complete buffer stack on flexible YSZ substrate.

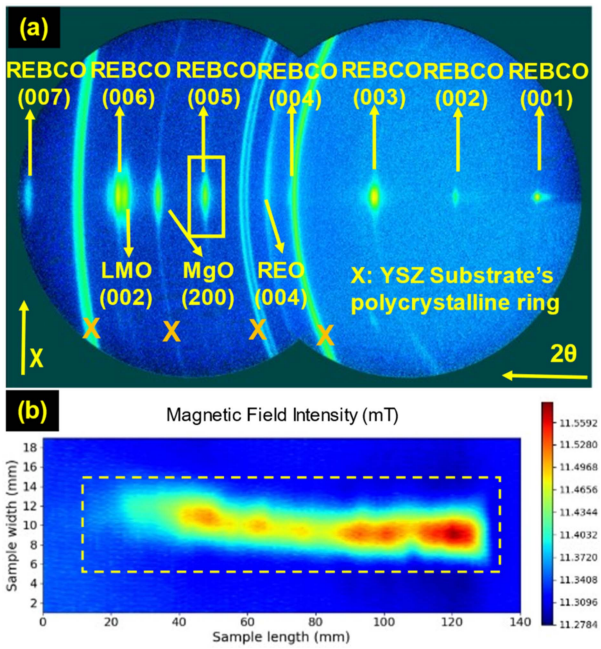

Fig. 3. (a) 2D XRD 2theta-omega scan from REBCO film on buffered flexible YSZ substrate, (b) remnant field map of REBCO/ buffered YSZ over sample length (inlet detailing the sample).

micrographs of an 8-cm-long dip-coated sample, taken after hard baking, are shown in Fig. 1. Measurements at four locations (A, B, C, and D) yielded an average R_a of 1.39 nm, indicating uniform surface roughness and suitability for further buffer layer growth. The thickness of planarization layer is approximately 500 nm.

A 10-nm-thick, biaxially-textured MgO (200) template was grown on an 8-nm Y_2O_3 layer after planarization. The sharp RHEED pattern of IBAD-MgO, shown in Fig. 2(a), confirms the good texture of the MgO film on the planarized flexible YSZ substrate. Subsequent homoepitaxial MgO layer ensures good crystallinity and promotes heteroepitaxy of the LMO cap layer. Fig. 2(b) illustrates a 2D XRD pattern of a buffer layer on a flexible YSZ substrate. The MgO and LMO layers exhibit excellent alignment, with sharp elliptical diffraction spots for MgO (200) and LMO (002) peaks, indicating the absence of misoriented grains. The polycrystalline rings are attributed to the YSZ substrate. The in-plane and out-of-plane textures of the LMO cap layer were measured to be 6.9° full width at half maximum (FWHM) and 3.9°FWHM, respectively. Misoriented grains in the LMO cap layer can lead to the formation of random-oriented/a-axis REBCO grains, negatively affecting superconducting performance. [26].

SEM cross-section of the complete buffer stack on the flexible YSZ shown in Fig. 2(c). The planarized film can be clearly seen to fill out the rough topology of the underlying YSZ substrate. Following the deposition of the buffer layer, the superconducting REBCO layer was grown by MOCVD, under conditions of temperature and oxygen partial pressure previously optimized and reported for flexible YSZ substrate [20].

2D XRD pattern (Fig. 3(a)) of REBCO grown on flexible YSZ reveals only (00l) reflections, suggesting c-axis oriented growth of REBCO film. The $\Delta\chi$ FWHM of REBCO (005) is recorded to be 2.59°. Furthermore, the visible peaks of MgO (200) and LMO (002), which align with the same zone axis as the REBCO peaks, validate the epitaxial nature of the REBCO thin film. The poly-crystalline rings are reflections from the YSZ substrate. The FWHM values on the 12-cm-long YSZ samples were slightly higher. This difference could be due to slightly higher in-plane and out-of-plane values of the buffer layer, along with other complex factors such as the composition of the REBCO film and the c-axis lattice parameter [27]. We expect the performance of the REBCO samples to improve after optimizing the growth parameters of both the buffer layer and the REBCO. To assess the critical current distribution in the REBCO samples, SHPM analysis was employed. This method enables the precise localization of defects within the REBCO tape [28]. The remnant field map for a 12-cm-long sample (Fig. 3(b)), demonstrates decent uniformity. We have successfully developed up to 12-cm-long

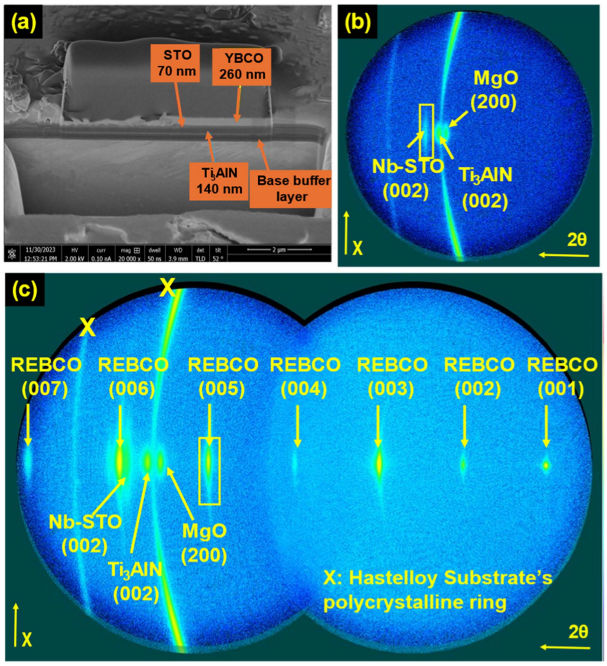

Fig. 4. (a) Cross-sectional SEM image of REBCO and conductive buffer substrate. (b) 2D XRD scans for the conductive buffer substrate. and (c) 2D XRD scans for the REBCO film grown on the conductive buffer layer.

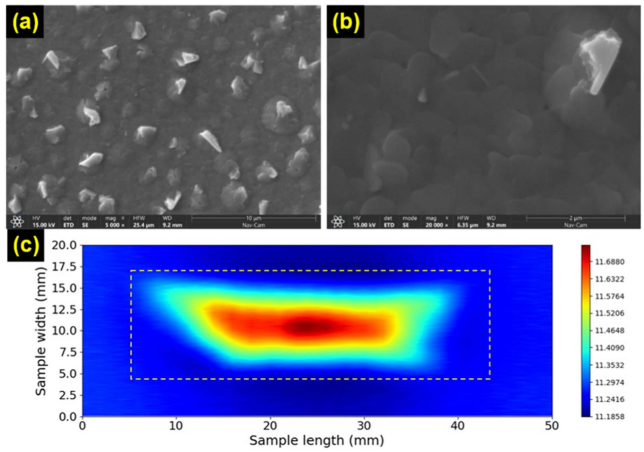

Fig. 5. SEM micrographs showing the surface morphology of a superconducting REBCO film grown on a conductive buffer substrate: (a) Low magnification and (b) high magnification. (c) Remnant field map of REBCO grown over conductive buffer (inlet detailing the sample).

flexible YSZ samples with a maximum critical current density of 1.08 MA/cm^2;.

Grain boundaries in HTS films have been identified as a key factor in reducing DC critical current densities and increasing surface resistance values, which contribute to microwave nonlinearities [29]. We have previously reported that superconducting REBCO films flexible YSZ substrates with high J_c values exceeding 1 MA/cm^2; exhibit R_s values of approximately 0.1 mΩ/square at 25 K and 9.4 GHz in short samples [20]. Detailed investigations into the Q-factor and RF applications of flexible, long-length samples will be included in future studies.

B. Growth of REBCO on Conductive Buffer Layer Over Metallic Substrate

The REBCO thin film was grown over a partially electrically-conductive buffer stack. Fig. 4(a) displays a cross-sectional view of the REBCO film along with the conductive buffer stack and 2D XRD plot of the conductive buffer layer is given in Fig. 4(b). The distinct elliptical diffraction spots corresponding to Nb-STO (002), Ti_3AlN (002), and MgO (200) peaks are clearly visible, signifying a well-aligned growth of the buffer layer. Furthermore, the lack of Nb-STO (110) peaks confirms the absence of misoriented grains in the Nb-STO cap layer, which is crucial for achieving a uniform and high-quality REBCO growth [30]. Fig. 4(c) illustrates the 2D XRD plot of REBCO grown over the buffer layer. The (00l) reflections of REBCO suggest a c-axis oriented growth of the REBCO film. Additionally, the visible peaks of Nb-STO (002), Ti_3AlN (002), and MgO (200) from the buffer layer, which align with the same zone axis as the REBCO peaks, validate the epitaxial nature of the REBCO thin film. Out-of-plane texture with a $\Delta\chi$ Full-width-at-half-maximum (FWHM) of REBCO (005) were measured to be 2.73°.

SEM micrographs of a REBCO film, with a J_c above 1 MA/cm^2;, grown on a conductive buffer structure are shown in the Fig. 5(a) and (b). The surface morphology of the REBCO layer reveals a smooth c-oriented film with some misaligned grains formation and possibly some secondary phases. We anticipate that these grains can be eliminated by optimizing the deposition temperature and film composition. Additionally, superconducting performance was evaluated using SHPM and critical current measurements. The remnant field map of a REBCO film grown on a conductive buffer sample measuring 4 cm in length is shown in Fig. 5(c). The maps show excellent uniformity of the coating along both the length and width. Critical current measurement at 77 K and 0 T on the REBCO tape reveals an I_c of 69 A (77 K, 0 T) for the full width of the sample (12 mm). This result confirms a successful REBCO film on a two-layer electrically conductive buffer, with a critical current density exceeding 1 MA/cm^2.

IV. Conclusion

In this study, we successfully developed high-quality REBCO superconducting thin films on 12-cm-long flexible YSZ substrates, achieving a critical current density (J_c) of 1.06 MA/cm^2; at 77 K, 0 T. The planarization of the YSZ surface to an average roughness $R_a < 2$ nm and the subsequent deposition of a biaxially-textured MgO template, followed by homo-epi MgO layer and a cap layer of $LaMnO_3$, resulted in good out-of-plane and in-plane texture values, facilitating excellent REBCO growth on the flexible YSZ substrate. Additionally, we advanced the development of an electrically conductive buffer architecture for defect-tolerant REBCO tapes, utilizing a Ti_3AlN buffer on Hastelloy C276 substrate with an Nb-STO cap layer. REBCO films grown on this buffer architecture also demonstrated a J_c greater than 1 MA/cm^2; at 77 K, self-field. These findings

highlight the potential of REBCO films on flexible substrates for microwave and radio frequency applications, as well as the effectiveness of conductive buffer architectures in enhancing the performance of REBCO tapes. Future work will focus on further optimizing the texture, microstructure, and composition to improve the critical current density and overall performance of REBCO superconductor tapes.

ACKNOWLEDGMENT

Manoj Thevalappilly Paulose fabricated REBCO tapes on flexible buffered YSZ and conductive buffer, Jithin Sai Sandra fabricated the buffered YSZ, Md Abu Sayeed developed conductive buffer template.

REFERENCES

[1] Y. Iijima, N. Tanabe, Y. Ikeno, and O. Kohno, "Biaxially aligned $YBa_2Cu_3O_{7-x}$ thin film tapes," *Physica C Supercond*, vol. 185–189, no. PART 3, pp. 1959–1960, Dec. 1991, doi: 10.1016/0921-4534(91)91104-C.

[2] N. Sekiya and Y. Monjugawa, "A novel REBCO wire structure that improves coil quality factor in MHz range and its effect on wireless power transfer systems," *IEEE Trans. Appl. Supercond.*, vol. 27, no. 4, Jun. 2017, Art. no. 6602005, doi: 10.1109/TASC.2017.2660058.

[3] D. Uglietti, "A review of commercial high temperature superconducting materials for large magnets: From wires and tapes to cables and conductors," *Supercond Sci Technol*, vol. 32, no. 5, Apr. 2019, Art. no. 053001, doi: 10.1088/1361-6668/AB06A2.

[4] W. Yang et al., "Accurate ruby sensor for stress analysis in electronics," *ACS Appl Electron Mater*, vol. 4, no. 9, pp. 4332–4339, Sep. 2022, doi: 10.1021/ACSAELM.2C00588/ASSET/IMAGES/MEDIUM/EL2C00588_0005.GIF.

[5] A. Bergen et al., "Design and in-field testing of the world's first ReBCO rotor for a 3.6 MW wind generator," *Supercond Sci Technol*, vol. 32, no. 12, Oct. 2019, Art. no. 125006, doi: 10.1088/1361-6668/AB48D6.

[6] M. Paidpilli and V. Selvamanickam, "Development of RE-Ba-Cu-O superconductors in the U.S. for ultra-high field magnets," *Supercond Sci Technol*, vol. 35, no. 4, Feb. 2022, Art. no. 043001, doi: 10.1088/1361-6668/AC5162.

[7] M. Omure, Y. Miyamoto, A. Ishiyama, W. Tomonori, and N. Shigeo, "Evaluation on applicability of no-insulation REBCO pancake coil to superconducting magnetic energy storage," *IEEE Trans. Appl. Supercond.*, vol. 31, no. 5, Aug. 2021, Art. no. 5700105, doi: 10.1109/TASC.2021.3058915.

[8] Y. Ji et al., "A Study about Ni–8 at % W alloy substrates used for REBCO coated conductors," *Phys. Met. Metallogr.*, vol. 122, no. 14, pp. 1473–1481, Dec. 2021, doi: 10.1134/S0031918X21140118.

[9] V. Selvamanickam, M. H. Gharahcheshmeh, A. Xu, E. Galstyan, L. Delgado, and C. Cantoni, "High critical currents in heavily doped $(Gd,Y)Ba_2Cu_3O_x$ superconductor tapes," *Appl Phys Lett*, vol. 106, no. 3, Jan. 2015, Art. no. 32601, doi: 10.1063/1.4906205/14464801/032601_1_ACCEPTED_MANUSCRIPT.PDF.

[10] A. Ghirri, C. Bonizzoni, D. Gerace, S. Sanna, A. Cassinese, and M. Affronte, "$YBa_2Cu_3O_7$ microwave resonators for strong collective coupling with spin ensembles," *Appl Phys Lett*, vol. 106, no. 18, May 2015, Art. no. 184101, doi: 10.1063/1.4920930.

[11] M. Morisue, J. Asahina, W. Lin, K. Yo, and N. Komine, "Fabrication of microstrip transmission line by high-T/sub c/superconducting materials," *IEEE Trans Magn*, vol. 27, no. 2, pp. 2801–2804, Mar. 1991, doi: 10.1109/20.133791.

[12] R. Weigel, A. A. Valenzuela, and P. Russer, "YBCO superconducting microwave components," *Appl. Supercond.*, vol. 1, no. 10–12, pp. 1595–1604, Oct. 1993, doi: 10.1016/0964-1807(93)90307-N.

[13] L.-M. Wang, W.-C. Lin, M.-L. Chang, C.-Y. Shiau, and C.-T. Wu, "Characteristics of ultra-wideband bandpass YBCO filter with impendence stub," *IEEE Trans. Appl. Supercond.*, vol. 21, no. 3, pp. 551–554, Jun. 2011, doi: 10.1109/TASC.2010.2091231.

[14] R. Nazifi et al., "Millimeter-wave response of all metal-organic deposited YBCO transition edge bolometer," *IEEE Trans. Appl. Supercond.*, vol. 31, no. 1, Jan. 2021, Art. no. 2100105, doi: 10.1109/TASC.2020.3033413.

[15] S. Ruffieux et al., "The role of kinetic inductance on the performance of YBCO SQUID magnetometers," *Supercond Sci Technol*, vol. 33, no. 2, Jan. 2020, Art. no. 025007, doi: 10.1088/1361-6668/ab6014.

[16] W. J. Carr Jr., "AC loss and macroscopic theory of superconductors," *CRC Press*, Jul. 5, 2001, doi: 10.1201/9781482264760.

[17] C. Pop et al., "High critical current solution derived $YBa_2Cu_3O_7$ films grown on sapphire," *Supercond Sci Technol*, vol. 35, no. 5, May 2022, Art. no. 054007, doi: 10.1088/1361-6668/ac5be9.

[18] Y. Zhang, S. Sun, R. Pratap, E. Galstyan, J. Wosik, and V. Selvamanickam, "Development of REBCO tapes on nonmetallic flexible substrates for RF applications," *IEEE Trans. Appl. Supercond.*, vol. 29, no. 5, Aug. 2019, Art. no. 3500405, doi: 10.1109/TASC.2019.2896545.

[19] J. S. Sandra et al., "Applications-oriented development of buffer architecture for REBCO films on nonmetallic substrates," *IEEE Trans. Appl. Supercond.*, vol. 33, no. 7, Oct. 2023, Art. no. 6602506, doi: 10.1109/TASC.2023.3289651.

[20] R. Jain, S. Sharma, J. S. Sandra, M. Y. Suarez Villagran, J. Wosik, and V. Selvamanickam, "Optimization of $REBa_2Cu_3O_{7-x}$ on flexible, dielectric substrates for high-frequency applications," *IEEE Trans. Appl. Supercond.*, vol. 33, no. 5, pp. 1–5, Aug. 2023, doi: 10.1109/TASC.2023.3251288.

[21] P. Gao, Y. Zhang, X. Wang, and Y. Zhou, "Interface properties and failures of REBCO coated conductor tapes: Research progress and challenges," *Superconductivity*, vol. 8, Dec. 2023, Art. no. 100068, doi: 10.1016/J.SUPCON.2023.100068.

[22] T. Aytug et al., "Growth and superconducting properties of $YBa_2Cu_3O_{7-\delta}$ films on conductive $SrRuO_3$ and $LaNiO_3$ multilayers for coated conductor applications," *Appl Phys Lett*, vol. 76, no. 6, pp. 760–762, Feb. 2000, doi: 10.1063/1.125886.

[23] R. Gartner et al., "High-J_c YBCO coated conductors based on IBAD-TiN using stainless steel substrates," *IEEE Trans. Appl. Supercond.*, vol. 21, no. 3, pp. 2920–2923, Jun. 2011, doi: 10.1109/TASC.2010.2080657.

[24] M. A. Sayeed, M. Paulose, J. S. Sandra, S. Sherin, A. Prabakaran, and V. Selvamanickam, "Development of electrically conductive buffer for REBCO conductor," *IEEE Trans. Appl. Supercond.*, 2024.

[25] J. R. Groves et al., "Improvement of IBAD MgO template layers on metallic substrates for YBCO HTS deposition," *IEEE Trans. Appl. Supercond.*, vol. 13, no. 2, pp. 2651–2654, Jun. 2003, doi: 10.1109/TASC.2003.811937.

[26] M. Dürrschnabel et al., "$La_{1-x}Mn_{1-y}O_{3\pm\delta}$ buffer layers on inclined substrate deposited MgO templates for coated conductors," *Supercond Sci Technol*, vol. 34, no. 3, Jan. 2021, Art. no. 035006, doi: 10.1088/1361-6668/ABD5F2.

[27] J. L. MacManus-Driscoll, J. A. Alonso, P. C. Wang, T. H. Geballe, and J. C. Bravman, "Studies of structural disorder in $ReBa_2Cu_3O_{7-x}$ thin films (Re = rare earth) as a function of rare-earth ionic radius and film deposition conditions," *Physica C Supercond*, vol. 232, no. 3–4, pp. 288–308, Nov. 1994, doi: 10.1016/0921-4534(94)90789-7.

[28] X. F. Li, M. Kochat, G. Majkic, and V. Selvamanickam, "Critical current density measurement of striated multifilament-coated conductors using a scanning Hall probe microscope," *Supercond Sci Technol*, vol. 29, no. 8, Jul. 2016, Art. no. 085014, doi: 10.1088/0953-2048/29/8/085014.

[29] D. E. Oates, H. Xin, G. Dresselhaus, and M. S. Dresselhaus, "Intermodulation distortion and Josephson vortices in YBCO bicrystal grain boundaries," *IEEE Trans. Appl. Supercond.*, vol. 11, no. 1, pp. 2804–2807, Mar. 2001, doi: 10.1109/77.919646.

[30] A. K. Jha and K. Matsumoto, "Superconductive REBCO thin films and their nanocomposites: The role of rare-earth oxides in promoting sustainable energy," *Front Phys*, vol. 7, no. JUN, Jun. 2019, Art. no. 449335, doi: 10.3389/FPHY.2019.00082/BIBTEX.